JMEPEG (2015) 24:2091–2098
DOI: 10.1007/s11665-015-1459-4

1059-9495/$19.00

Analysis of Microstructure and Texture Evolution in Mg-3Al-1Zn Alloy Processed Through Groove Rolling

S.V.S. Narayana Murty, Niraj Nayan, R. Madhavan, S.C. Sharma, K.M. George, and Satyam Suwas

(Submitted December 14, 2014; in revised form January 29, 2015; published online March 7, 2015)

The mechanism of grain refinement in a AZ31 Mg alloy subjected to hot groove rolling is investigated up to large strain ($\varepsilon_t \sim 2.5$). The alloy shows enhanced yield strength without compromising ductility. The change in strain path during rolling has resulted in significant weakening of basal texture. The microstructure analyses show that dynamic recrystallization (DRX) contributed significantly to grain refinement and hence to the observed mechanical properties. The combined effects of DRX and texture evolution on mechanical properties have been addressed.

Keywords AZ31 alloy, dynamic recrystallization, groove rolling, texture

1. Introduction

Magnesium alloys are attractive for lightweight structural applications in the aerospace industry because of their low density and high specific strength and stiffness (Ref 1). Most of the wrought alloys of magnesium are based on Mg-Al-Zn-Mn system. These alloys usually contain between 0 and 8 wt.% aluminum for room-temperature strength, while zinc is maintained between 0 and 1.5 wt.% to limit hot shortness during thermo-mechanical processing (Ref 2). Magnesium has hexagonal close-packed crystal structure with a *c*/*a* ratio of 1.623, which is close to the ideal packing value (1.633), and exhibits limited number of independent slip systems at room temperature. At ambient temperature, basal slip is the predominant contributor to plastic deformation. However, at elevated temperatures, the critical resolved shear stress (CRSS) for prismatic and pyramidal slip systems reduces, thus enhancing the workability of Mg alloys (Ref 3). The workability of Mg alloys, at room temperature, can be improved by the refinement of grain size which gives rise to a better combination of strength and ductility at room temperature (Ref 4-6). This phenomenon has been attributed to the following causes: (i) in a coarse-grained Mg alloy, the number of slip systems that are activated near the grain boundaries is more (both basal and non-basal) so as to maintain the plastic compatibility with neighboring grains compared to the grain interior, where only basal slip system is active. However, with decreasing grain size, these grain boundary zones would extend up to the grain interior, and hence both basal and non-basal slip systems would be active within the whole grain (Ref 7); (ii) higher critical stress needed for crack propagation along the grain boundaries. The large fraction of grain boundaries in fine-grained alloys offers a tortuous path for cracks to propagate to fracture, thus accommodating large strain to failure (Ref 8).

The ductility of magnesium alloys is strongly affected by two main factors: (1) development of strong textures during processing and (2) deformation by limited number of slip and twin systems. It has been reported that the critical resolved shear stress (CRSS) for basal plane slip in magnesium single crystal exhibits 100 times lower value than that for non-basal slip near room temperature (Ref 9, 10). Thus, the distribution of basal poles in magnesium alloy plays an important role in the enhancement of mechanical properties at room temperature. In addition, the ultra-fine-grained Mg alloys are shown to exhibit superplasticity at high strain rates and at relatively lower temperatures (Ref 11, 12). In large-grained Mg alloys, apart from basal slip, twinning is the common deformation mode at room temperature that is generally observed from very early stages of deformation (Ref 13). The ductility of HCP metals is reported to have enhanced by the presence of twins in microstructure (Ref 14). Since the tendency for twinning decreases with reducing grain size, the activity of this mode is compensated by the activation of non-basal slip systems (Ref 7, 15, 16).

The fine-grained magnesium alloys exhibit lower ductile-to-brittle transformation temperature (DBTT). The DBTT of Mg is 250 °C for a grain size of 60 μm, which reduces to room temperature when the grain size is reduced to 2 μm. This low temperature ductility has been attributed to the transition in the fracture mechanism from intergranular to transgranular nature (Ref 17).

Apart from grain size, the other variable that governs the plastic workability of Mg alloys is its crystallographic texture. Conventionally processed Mg alloys show a dominant basal texture, i.e., most of the grains have their {0001} plane parallel to the normal plane (Ref 18). The materials with such texture are difficult to process subsequently since the resolved shear stress acting on the basal plane is almost zero. Therefore, it is important to develop methods for producing alloys with weaker basal texture so as to attain better formability and reduce in-plane anisotropy of the rolled sheet (Ref 19). The change in strain path during deformation has been found to be an efficient way to reduce the intensity of basal texture (Ref 20, 21). The

S.V.S. Narayana Murty, Niraj Nayan, S.C. Sharma, and **K.M. George**, Materials and Metallurgy Group, Materials and Mechanical Engineering Entity, Vikram Sarabhai Space Center, Trivandrum 695 022, India; and **R. Madhavan and Satyam Suwas**, Department of Materials Engineering, Indian Institute of Science, Bangalore 560012, India. Contact e-mails: maddy.iisc@gmail.com and satyamsuwas@materials.iisc.ernet.in.

effect of strain path change on the evolution of texture and microstructure has been widely studied in various FCC (Ref 22) and HCP (Ref 23) crystal systems during rolling. It is observed that specimens subjected to multi-directional rolling process exhibit similar grain morphologies as that of uni-directional rolling but different crystallographic textures.

Mg-3Al-1Zn alloy (AZ31) is one of the most commonly used wrought magnesium alloy and has attracted the attention of researchers worldwide. The objective of the present investigation is to carry out texture engineering in AZ31 alloy as a function of strain path change through a variant of rolling process, i.e., groove rolling. The technique involves the rotation of sample about the rolling direction (RD) after each successive pass. The present paper correlates the evolution of crystallographic texture and microstructure in AZ31 magnesium alloy processed by multi-step hot groove rolling.

2. Experiments

2.1 Material and Processing

The material used in the present study is AZ31 magnesium alloy (Mg-3Al-1Zn-0.2Mn, all in weight percent). The starting material is obtained in hot-forged condition. Blocks of size $200 \times 45 \times 45$ mm were sectioned from the forged stock and section rolled at 250 and 300 °C to $L \times 12 \times 12$ mm imposing a total thickness reduction of ~92% ($\varepsilon \sim 2.5$), through a series of roll passes in a grooved rolling mill (Fig. 1a). The groove rolling mill used in the present study has series of grooves with diamond-shaped slots for the passage of workpiece. The cross section of the workpiece inserted into the groove assumes its shape (Fig. 1b). The strain per pass can be controlled by manipulating the height of the rolls, and the rolling is carried out by inserting the workpiece through a series of slots with gradually decreasing sizes. The samples were heated in an electrical billet heating furnace with an accuracy of ±5 °C. The normal direction of the specimen was changed in increments of 90° by rotation about the rolling direction after each pass. Intermediate heating between rolling passes was done for 15 min to maintain the temperature of the billet. The rolled rods were subjected to microstructure, texture, and mechanical property characterization, after discarding 100 mm from either ends.

2.2 Characterization and Testing

For optical microscopy, samples were prepared by conventional metallographic techniques using a series of emery papers followed by polishing with 3 micron diamond paste. The as-polished surfaces were etched with acetic picral for 5 s. The mechanical property evaluation was carried out by tension test at a strain rate of 10^{-3}/s. Circular cross-section specimens with a gage length of 25 mm and a diameter of 10 mm were cut along the length of the rolled rods. Bulk textures for initial and rolled samples were measured on the normal plane (ND) (Fig. 1b) using a Panalytical Xpert texture goniometer with Cu K_α radiation. (002), (110), (102), and (103) pole figures were measured up to 75° radial angle (α). Orientation Distribution Function (ODF) has been calculated from the experimental pole figures using Labotex® software based on Arbitrarily Defined Cells (ADC) algorithm. Microstructure and micro-texture measurements were carried using an FEI Quanta scanning electron microscope attached with an electron back-scattered

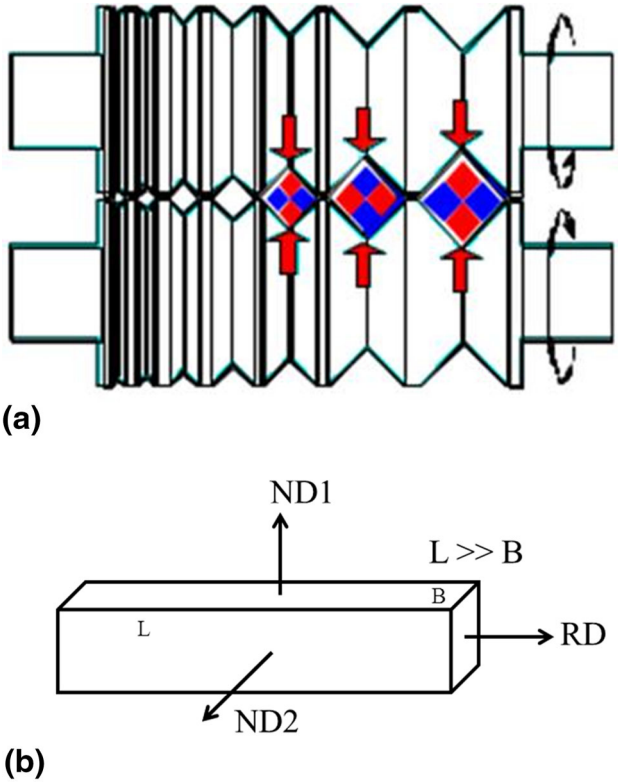

Fig. 1 Schematic of (a) groove rolling mill, (b) sample direction conventions used in the present study

diffraction facility. All the scans were obtained on the plane perpendicular to rolling direction (RD). TSL OIM 6 data collection and analysis software was used to collect and process the orientation information. Inverse pole figures (IPF) and ODF corresponding to the RD plane were calculated from the EBSD-generated orientation imaging microscopy (EBSD-OIM) maps.

3. Results and Discussion

3.1 Microstructure

3.1.1 Optical Microscopic Observation. The microstructure of the initial hot-forged material is shown in Fig. 2a, which reveals a coarse-grained structure with an average grain size of about 200 μm and a large fraction of twins. Figure 2(b)-(e) shows the optical micrographs for the samples groove rolled at 250 and 300 °C, obtained from the planes perpendicular to the longitudinal (ND) and rolling (RD) directions. The comparison of warm-rolled and initial forged microstructures indicates that the hot groove rolling results in a significant reduction in grain size. The coarse-grained initial microstructure transforms to an equiaxed, fine-grained structure after groove rolling. The fraction of twins observed in the rolled microstructure is significantly less compared to the initial as-forged material.

3.1.2 Microstructural Observation by Electron Backscatter Diffraction (EBSD). Figure 3(a)-(d) shows the EBSD-generated orientation image micrographs and the corresponding grain boundary maps for the deformed samples. The microstructures are qualitatively similar at both the rolling

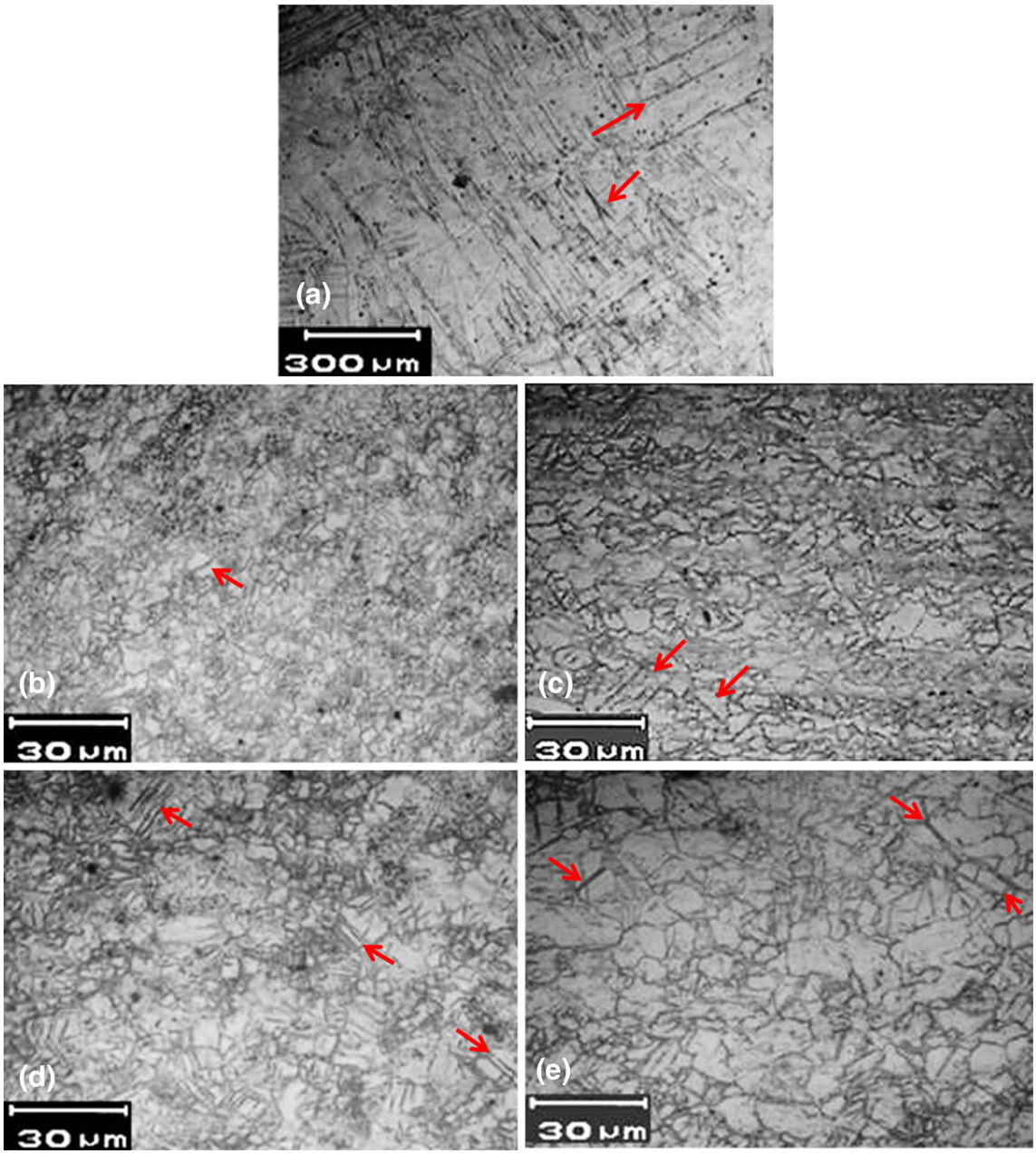

Fig. 2 Optical photomicrographs of (a) starting forged block used in this study; (b, c) after rolling at 250 °C; (d, e) after rolling at 300 °C with (b, d) taken in cross section and (c, e) taken along the longitudinal section of the bar. Highlighted regions indicate some of the deformation twin traces

temperatures; however, the fraction of fine equiaxed grains is higher at 300 °C than at 250 °C. It is known that basal slip is the dominant deformation mode in magnesium alloys at any given temperature (Ref 24). However, if the starting material has predominant fraction of basal-oriented grains, then further processing would be difficult as the resolved shear stress acting on the basal slip planes would be zero. This can be overcome by two ways: (1) by increasing the temperature of deformation, so that CRSS for other slip systems can be reduced; or (2) by activation of twinning systems. A sharp reorientation of the parent matrix caused by twinning could facilitate slip in the twinned region subsequently. In Mg alloys, two types of twinning modes are observed, (i) tensile twinning and (ii) contraction twinning. The former reorients the parent orientation by 86° about $\langle 11\ \bar{2}0\rangle$, and the latter causes 56° reorientation about $\langle 11\ \bar{2}0\rangle$ (Ref 25). The grain boundary maps show that twinning is active at 250 °C (twin boundaries being highlighted), apart from the other commonly operative slip modes at high temperatures (Fig. 3b). At 300 °C, the fraction of twin boundary traces is lesser than at 250 °C which implies that slip-based deformation process is dominant (which is also inferred from the orientation gradients within grains, Fig. 3a and c).

Figure 4(a)-(c) shows various microstructural features obtained from the orientation maps. The grain size distribution followed a log-normal function for both the rolling conditions. There is no significant variation in grain sizes with rolling temperatures. The wider grain size distribution in both cases is

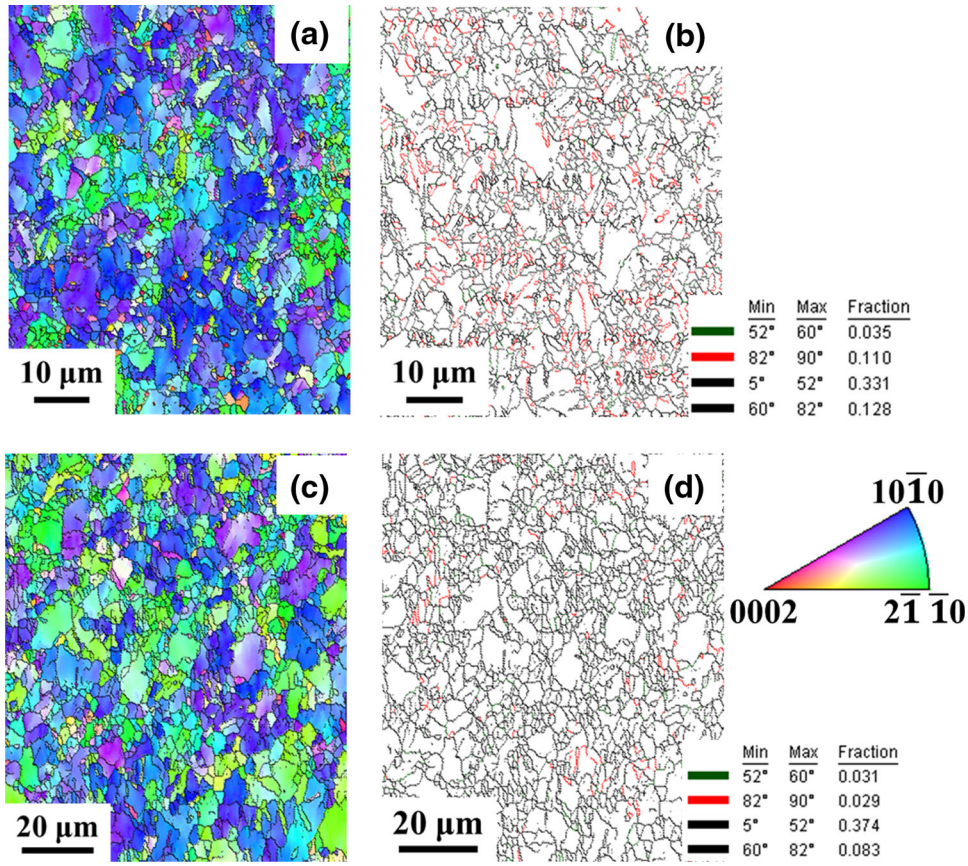

Fig. 3 Orientation image and grain boundary maps for section-rolled samples. (a, b) 250 °C, (c, d) 300 °C. Extension twin boundaries are highlighted in red and contraction twin boundaries are in green for both the cases (Color figure online)

attributed to the combined presence of DRX and deformed grains. The distribution of misorientation angles across the grain boundaries shows that the value peaked at around 85° for 250 °C rolled sample. This value corresponds to the misorientation angle that tensile twins make with the parent matrix (Fig. 3b and d, and 4b). However, this peak has fallen sharply at 300 °C, indicating that the activity of twinning has reduced significantly. The misorientation profile also shows a slight hump at ~30° at 250 °C and a more prominent one at 300 °C. This misorientation is generally attributed to the in-plane rotation of DRX grains with respect to deformed parent matrix (Ref 26). Hence, based on the above observations, it can be inferred that there exists a transition in deformation mechanisms from significant twin activity at 250 °C to dominant slip mode at higher temperatures. Figure 4(c) illustrates the kernal average misorientation (KAM) which is a measure for local misorientation build-up. KAM at any given pixel is defined as the mean of misorientation between its nearest neighbor pixels. KAM values can be correlated with strain accumulation in the microstructure (Ref 27). Here, the KAM is calculated between the first nearest neighboring pixels. The KAM distributions at 250 and 300 °C show almost overlapping profiles, implying that there is no significant variation in terms of dislocation storage in the microstructure at these processing temperatures. This observation led to an understanding that continuous dislocation annihilation occurs during deformation. This phenomenon can be attributed to two reasons: (1) high deformation temperature and (2) change in strain path. Changing the strain path, by the physical rotation of sample, leads to the activation of new set of slip systems. The dislocations that are generated encounter the forest of dislocations that are created during the previous strain path which promotes dynamic recovery (Ref 28).

Figure 5 shows the axis-angle pair of misorientation between neighboring pixels plotted in IPF triangle for the rolled samples. The high density of points clustered around ⟨11 $\bar{2}$0⟩ axis in the 85° IPF triangle at 250 °C corresponds to the misorientation caused by tensile twinning (Fig. 5a). However, the density of points around 85°/⟨11 $\bar{2}$0⟩ is lesser at 300 °C indicating that the activation of twinning has subsided (Fig. 5b).

3.2 Texture

Figure 6(a) and (b) shows the 001 inverse pole figures for the rolled samples, as obtained from the EBSD-OIM maps. Since groove rolling can be considered similar to extrusion process, inverse pole figure (IPF) corresponding to RD plane, which is equivalent to extrusion plane, has been displayed. The sample maintained the square cross section throughout the rolling process, owing to the sample rotation about RD after each pass. Hence, the ND and TD planes can be considered similar. IPF for 250 °C shows strong intensity near 10 $\bar{1}$0 poles, which implied that most of the grains are oriented with its ⟨10 $\bar{1}$0⟩ directions parallel to the rolling direction, a common observation in Mg alloys during extrusion (Ref 29). However, the texture becomes weak and starts to scatter towards ⟨11 $\bar{2}$0⟩ at 300 °C, which is due to dynamic recrystallization.

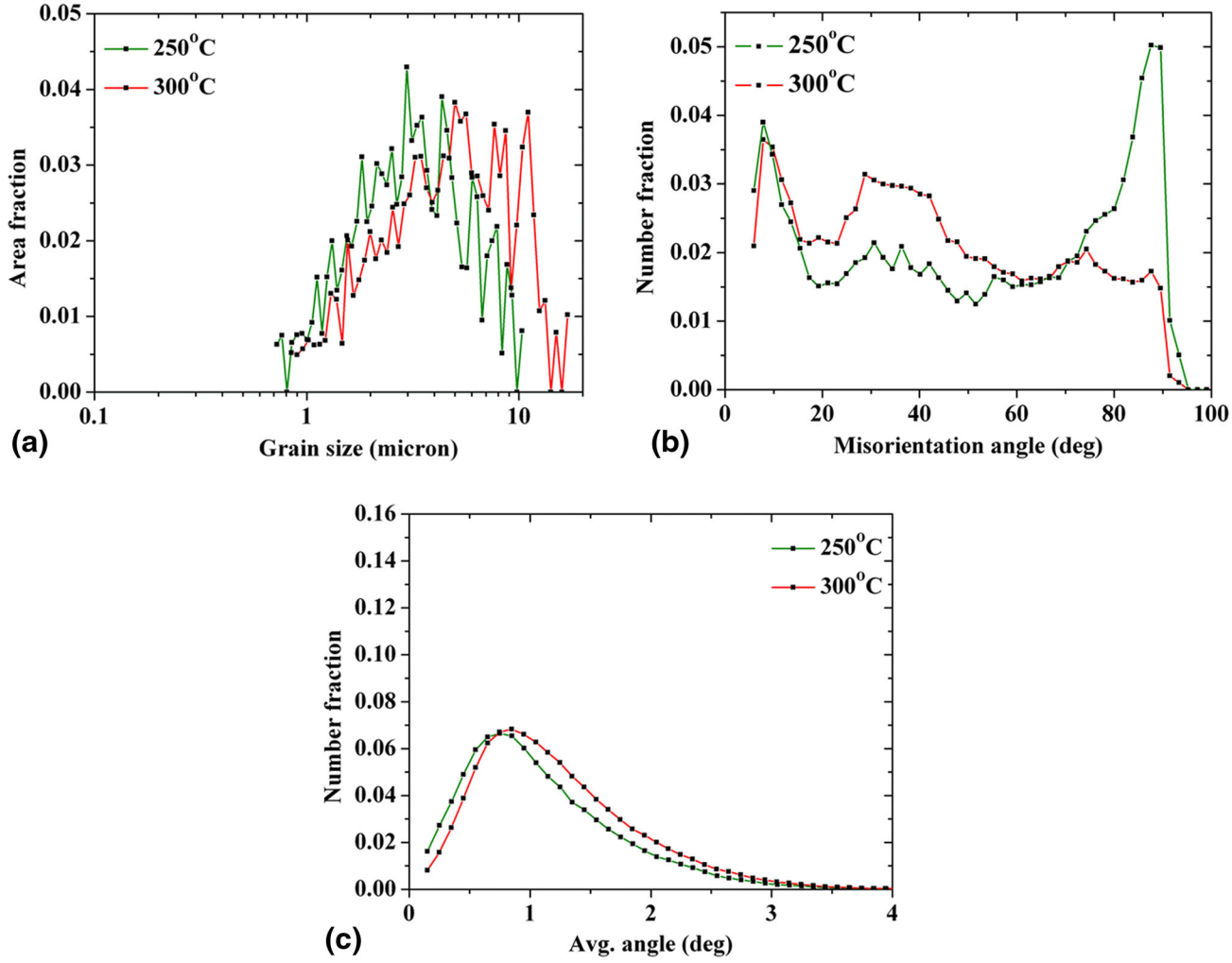

Fig. 4 Grain size and local misorientation information obtained from EBSD orientation maps for the rolled samples: (a) grain size distribution, (b) grain boundary misorientation profile, and (c) kernel average misorientation plot

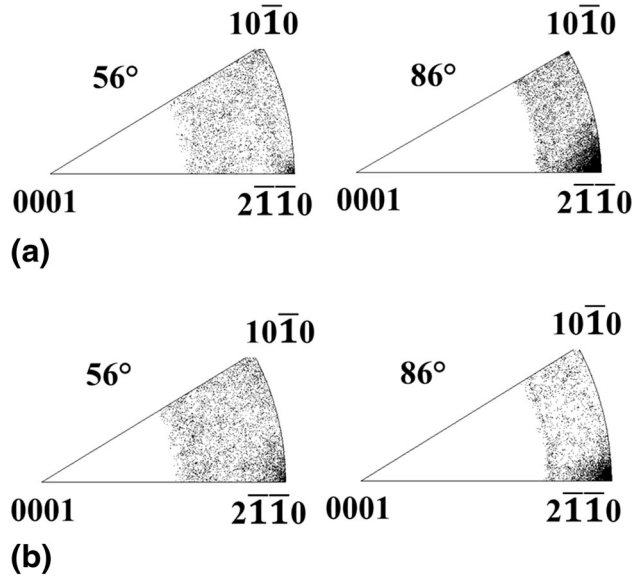

Fig. 5 Axis-angle plot, calculated from the EBSD-generated orientation image maps, shown in 55°, 85° IPF triangles. (a) 250 °C, (b) 300 °C

Figure 7 shows the $\varphi_2 = 0°$, 30° sections of the ODF corresponding to RD plane, as calculated from the orientation maps. The $\varphi_2 = 0°$ section shows a continuous fiber along φ_1 from 0° to 180° at $\Phi = 90°$. With increasing temperature, an increase in texture intensity is observed in the $\varphi_2 = 30°$ section, whereas a reduction is found in $\varphi_2 = 0°$ section. Biswas et al. (Ref 30) have earlier reported, by comparing the experimental and simulated textures, that the advent of DRX during high-temperature deformation of Mg alloys causes the texture intensity to show up in $\varphi_2 = 30°$ section. This implied that higher texture intensity at 300 °C than at 250 °C in $\varphi_2 = 30°$ section is attributed to textural change due to DRX. Since DRX is associated with a rotation of 30° about the c-axis (Ref 26), the increase in intensity is associated with DRX. This observation is concordant with the earlier observation implied from the EBSD misorientation angle plot which shows a slight hump at 30° (Fig. 4b). Ion et al. (Ref 24) proposed that when a basal axis is tilted away from the compression axis, slip on the basal planes will lead to lattice rotation and results in sub-grains formation subsequently to the nucleation of DRX grains. The texture change during DRX in Mg alloys is difficult to observe in {00.2} pole figure as the rolling plane remains basal {00.1} after recrystallization (Ref 31).

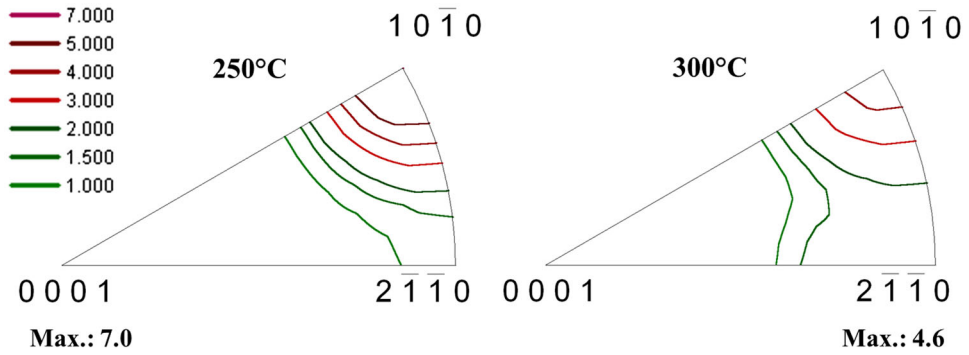

Fig. 6 RD inverse pole figures for the rolled samples. **(a)** 250 °C, **(b)** 300 °C

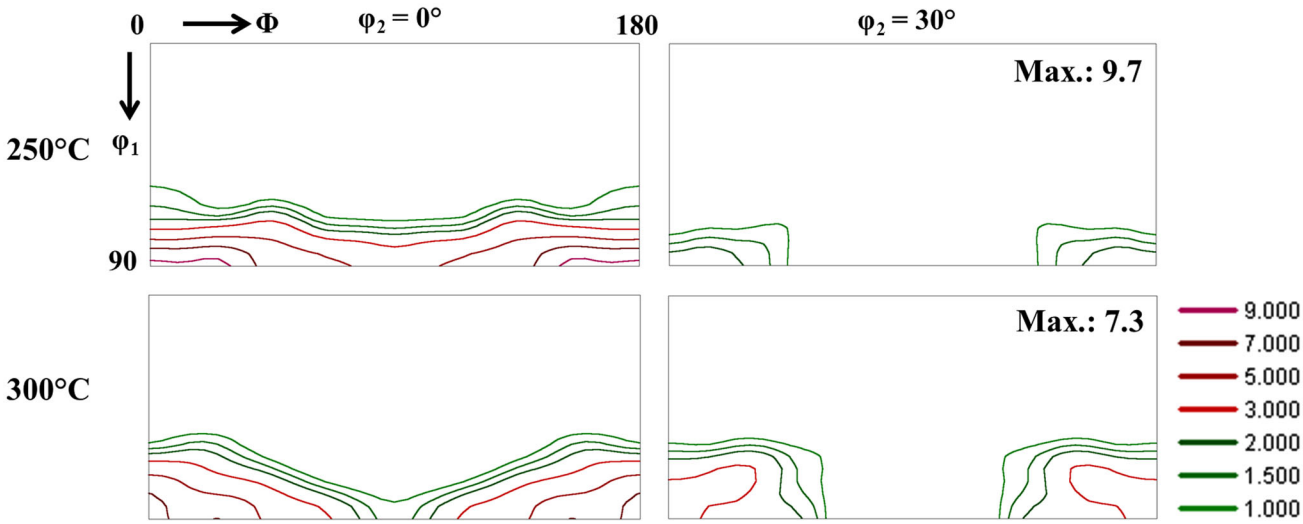

Fig. 7 ODF sections (φ_2 = 0°, 30°) for the as-forged and hot-rolled materials corresponding to RD plane

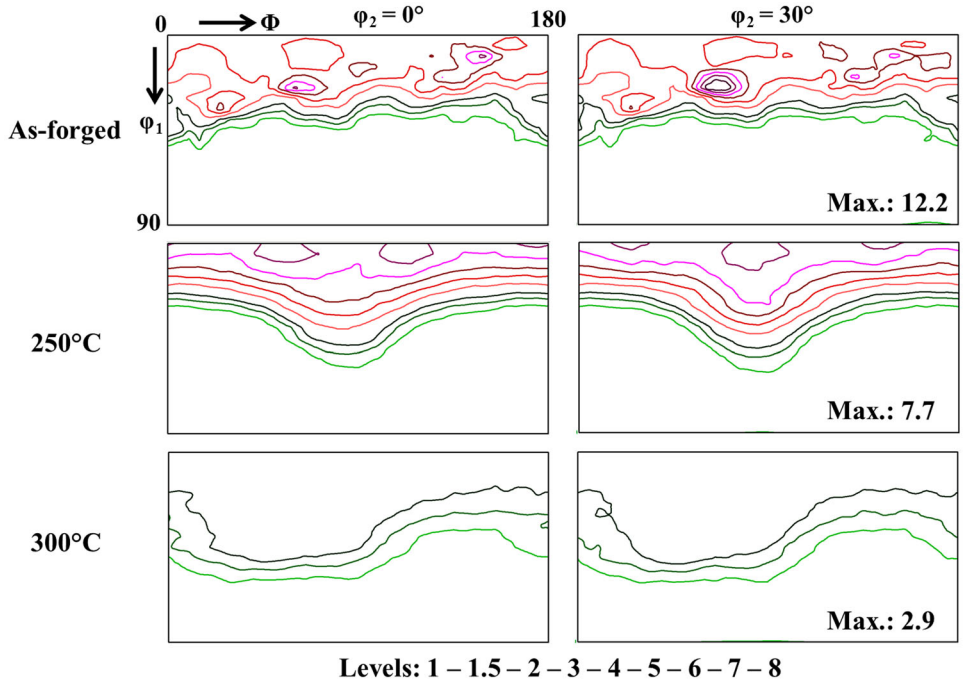

Fig. 8 ODF sections (φ_2 = 0°, 30°) for the as-forged and hot-rolled materials corresponding to ND plane

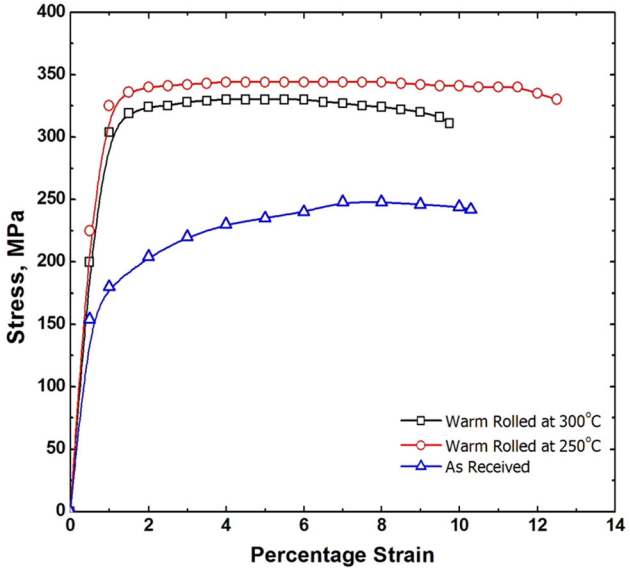

Fig. 9 Stress-strain curves for the initial as-forged material and groove-rolled samples

The ODF calculated (obtained from x-ray pole figure measurements) on the ND plane of the samples develop a weak basal fiber with increasing rolling temperature (Fig. 8). The initial forged material shows a strong near-basal texture. The weakening of basal poles during rolling can be attributed to the following reasons: (i) physical rotation of the sample about RD during each pass; the rotation causes the basal poles to oscillate towards ND1 or ND2 and hence prevents it from attaining a stable basal position which otherwise could have led to strong texture evolution (Ref 28) and (ii) higher activity of pyramidal $\langle c + a \rangle$ slip at elevated temperature which tends to tilt the basal poles away from the loading axis (Ref 18).

3.3 Dynamic Recrystallization Mechanisms

Ion et al. (Ref 24) have proposed a rotational recrystallization mechanism for DRX in Mg alloys for deformation temperatures less than 600 K, which attributes recrystallization to heterogeneity in plastic deformation near the grain boundaries with respect to grain interiors. It is proposed that gradual rotation of sub-grains near the grain boundaries by dislocation accumulation leads to the build-up of misorientation, eventually leading to the formation of new grains. Since in this process nucleation and growth are difficult to distinguish, it is referred to as continuous dynamic recrystallization (CDRX) and is associated with extensive cross-slip. CDRX is always associated with recrystallized orientations similar to that of deformed matrix. Another type of DRX mechanism observed at large strains and high temperatures where grain boundary migration is faster than sub-grain transformation is referred to as discontinuous dynamic recrystallization (DDRX), which is mainly accompanied by dislocation climb (Ref 32). In the present case, the DRX grains follow the orientations of parent matrix and are not associated with any additional texture peaks, which is a typical characteristic of CDRX (Ref 33).

3.4 Mechanical Properties

Figure 9 shows the stress-strain plot for the groove-rolled samples at 250 and 300 °C along with the initial as-forged material. It can be seen that the yield strengths of the rolled samples are more than twice that of the starting material. The samples rolled at 250 and 300 °C show yield strength of 275 and 325 MPa and a fracture strain of 12 and 10%, respectively. This significant improvement in mechanical properties is attributed to the fine-grained microstructure in the groove-rolled specimens. The combination of enhanced ductility and better yield strength is attributed to the combined effect of smaller grain size, strain homogeneity, and suitable deformation texture (Ref 34).

4. Conclusions

The following are the important observations on the texture-microstructure-mechanical properties correlation in AZ31 magnesium alloy processed by multi-pass groove rolling:

- Multi-pass warm groove rolling led to the modification of the initial twinned and coarse-grained microstructure into a uniform fine-grained microstructure.
- The grain sizes of 5 and 8 μm are obtained from the initial 200 μm by groove rolling at 250 and 300 °C, respectively.
- The change in strain path has resulted in a significant weakening of initial basal texture with increasing rolling temperature.
- The occurrence of dynamic recrystallization does not lead to the formation of any additional texture peak, and the DRX grains follow the orientations of the parent grains.
- From the misorientation plot of deformed samples, extension twinning has been found to be more favorable than the contraction twins. However, twinning tendency reduces with increasing rolling temperature.
- The yield strength and strain to fracture enhance as a result of grain refinement and texture evolution.

Acknowledgment

The authors acknowledge the help extended by Mr. K P Prakash and Mr. S. Manwatkar of Materials and Metallurgy Group, Vikram Sarabhai Space Centre (VSSC), during the alloy processing and metallographic characterization, respectively. The authors are also grateful to Director (VSSC) for encouragement and permission to publish this work.

References

1. K.U. Kainer and F. Kaiser, *Magnesium Alloys and Technology*, Wiley, Weinheim, 2003
2. M.M. Avedesian and H. Baker, *ASM Specialty Handbook: Magnesium and Magnesium Alloys*, ASM International, Materials Park, 1999
3. P. Patridge, Magnesium Alloys and Its Applications, *Metall. Rev.*, 1967, **118**, p 169–178
4. K. Kubota, M. Mabuchi, and K. Higashi, Review Processing and Mechanical Properties of Fine-Grained Magnesium Alloys, *J. Mater. Sci.*, 1999, **34**(10), p 2255–2262
5. S. Suwas, G. Gottstein, and R. Kumar, Evolution of Crystallographic Texture During Equal Channel Angular Extrusion (ECAE) and Its Effects on Secondary Processing of Magnesium, *Mater. Sci. Eng. A*, 2007, **471**(1–2), p 1–14

6. S. Biswas, S.S. Dhinwal, and S. Suwas, Room-Temperature Equal Channel Angular Extrusion of Pure Magnesium, *Acta Mater.*, 2010, **58**(9), p 3247–3261
7. J. Koike, T. Kobayashi, T. Mukai, H. Watanabe, M. Suzuki, K. Maruyama, and K. Higashi, The Activity of Non-basal Slip Systems and Dynamic Recovery at Room Temperature in Fine-Grained AZ31B Magnesium Alloys, *Acta Mater.*, 2003, **51**(7), p 2055–2065
8. T. Mohri, M. Mabuchi, N. Saito, and M. Nakamura, Microstructure and Mechanical Properties of a Mg-4Y-3RE Alloy Processed by Thermo-Mechanical Treatment, *Mater. Sci. Eng. A*, 1998, **257**(2), p 287–294
9. T. Obara, H. Yoshinga, and S. Morozumi, {1122} <1123> Slip System in Magnesium, *Acta Metall.*, 1973, **21**(7), p 845–853
10. J.F. Stohr and J.P. Poirier, Electron-Microscope Study of Pyramidal Slip 1122 <1123> in Mg, *Philos. Mag.*, 1972, **25**(6), p 1313–1329
11. H. Watanabe, T. Mukai, K. Ishikawa, and K. Higashi, Low Temperature Superplasticity of a Fine-Grained ZK60 Magnesium Alloy Processed by Equal-Channel-Angular Extrusion, *Scr. Mater.*, 2002, **46**(12), p 851–856
12. M. Mabuchi, K. Ameyama, H. Iwasaki, and K. Higashi, Low Temperature Superplasticity of AZ91 Magnesium Alloy with Non-equilibrium Grain Boundaries, *Acta Mater.*, 1999, **47**(7), p 2047–2057
13. R.W. Hertzberg, *Deformation and Fracture Mechanics of Engineering Materials*, Wiley, New York, 1976
14. M.H. Yoo, Slip, Twinning, and Fracture in Hexagonal Close-Packed Metals, *Metall. Trans. A*, 1981, **12**(3), p 409–418
15. N. Ecob and B. Ralph, The Effect of Grain Size on Deformation Twinning in a Textured Zinc Alloy, *J. Mater. Sci.*, 1983, **18**(8), p 2419–2429
16. M.A. Meyers, O. Vöhringer, and V.A. Lubarda, The Onset of Twinning in Metals: A Constitutive Description, *Acta Mater.*, 2001, **49**(19), p 4025–4039
17. T. Mukai, T. Mohri, M. Mabuchi, M. Nakamura, K. Ishikawa, and K. Higashi, Experimental Study of a Structural Magnesium Alloy with High Absorption Energy Under Dynamic Loading, *Scr. Mater.*, 1998, **39**(9), p 1249–1253
18. S.R. Agnew, M.H. Yoo, and C.N. Tome, Application of Texture Simulation to Understanding Mechanical Behavior of Mg and Solid Solution Alloys Containing Li or Y, *Acta Mater.*, 2001, **49**, p 4277–4289
19. E. Yukutake, J. Kaneko, and M. Sugamata, Anisotropy and Non-uniformity in Plastic Behavior of AZ31 Magnesium Alloy Plates, *Mater. Trans. JIM*, 2003, **44**(4), p 452–457
20. M.Y. Huh, S.Y. Cho, and O. Engler, Randomization of the Annealing Texture in Aluminum 5182 Sheet by Cross-Rolling, *Mater. Sci. Eng. A*, 2001, **315**(1), p 35–46
21. S. Suwas and A.K. Singh, Role of Strain Path Change in Texture Development, *Mater. Sci. Eng. A*, 2003, **356**(1), p 368–371
22. N.P. Gurao, S. Sethuraman, and S. Suwas, Effect of Strain Path Change on the Evolution of Texture and Microstructure During Rolling of Copper and Nickel, *Mater. Sci. Eng. A*, 2011, **528**(25), p 7739–7750
23. N.P. Gurao, A. Ali, and S. Suwas, Study of Texture Evolution in Metastable β-Ti Alloy as a Function of Strain Path and Its Effect on α Transformation Texture, *Mater. Sci. Eng. A*, 2009, **504**(1), p 24–35
24. S.E. Ion, F.J. Humphreys, and S.H. White, Dynamic Recrystallisation and the Development of Microstructure During The High Temperature Deformation of Magnesium, *Acta Metall.*, 1982, **30**(10), p 1909–1919
25. R. Abbaschian, L. Abbaschian, and R.E. Reed-Hill, *Physical Metallurgy Principles*, Cengage Learning, Stamford, 2008
26. F.J. Humphreys and M. Hatherly, *Recrystallization and Related Annealing Phenomena*, Pergamon, Oxford, 2004
27. A.J. Schwartz, M. Kumar, B.L. Adams, and D.P. Field, *Electron Backscatter Diffraction in Materials Science*, Springer, New York, 2009
28. T. Al-Samman and G. Gottstein, Influence of Strain Path Change on the Rolling Behavior of Twin Roll Cast Magnesium Alloy, *Scr. Mater.*, 2008, **59**(7), p 760–763
29. J. Bohlen, S.B. Yi, D. Letzig, and K.U. Kainer, Effect of Rare Earth Elements on the Microstructure and Texture Development in Magnesium–Manganese Alloys During Extrusion, *Mater. Sci. Eng. A*, 2010, **527**, p 7092–7098
30. S. Biswas, S. Suwas, R. Sikand, and A.K. Gupta, Analysis of Texture Evolution in Pure Magnesium and the Magnesium Alloy AM30 During Rod and Tube Extrusion, *Mater. Sci. Eng. A*, 2011, **528**(10), p 3722–3729
31. T. Al-Samman and G. Gottstein, Dynamic Recrystallization During High Temperature Deformation of Magnesium, *Mater. Sci. Eng. A*, 2008, **490**(1), p 411–420
32. A. Galiyev, R. Kaibyshev, and G. Gottstein, Correlation of Plastic Deformation and Dynamic Recrystallization in Magnesium Alloy ZK60, *Acta Mater.*, 2001, **49**(7), p 1199–1207
33. S. Biswas, D.-I. Kim, and S. Suwas, Asymmetric and Symmetric Rolling of Magnesium: Evolution of Microstructure, Texture and Mechanical Properties, *Mater. Sci. Eng. A*, 2012, **550**, p 19–30
34. S. Biswas and S. Suwas, Evolution of Sub-Micron Grain Size and Weak Texture in Magnesium Alloy Mg–3Al–0.4Mn by a Modified Multi-axial Forging Process, *Scr. Mater.*, 2012, **66**(2), p 89–92